THREE-DIMENSIONAL FIB-OIM OF CERAMIC MATERIALS

Shen J. Dillon
Carnegie Mellon University
5000 Forbes Avenue
Pittsburgh, Pa 15213

Gregory S. Rohrer
Carnegie Mellon University
5000 Forbes Avenue
Pittsburgh, Pa 15213

ABSTRACT

Three-dimensional characterization of materials is important for understanding and predicting their microstructural evolution and properties. Traditional serial sectioning of bulk samples is difficult, tedious, and not well suited for fined grained materials. In recent years, the dual-beam focused ion beam microscope has allowed for the prospect of three-dimensional characterization of fine grained materials to be performed more routinely. However, limited work has been performed on ceramics. Examples of three-dimensional reconstruction of orientation image maps from electron backscatter diffraction patterns are given for yttria-stabilized zirconia, alumina, strontium titanate and spinel.

INTRODUCTION

Obtaining three-dimensional (3-D) microstructural information is an important step in accurately quantifying the structural characteristics of polycrystals. In many cases, stereology provides useful statistical information for grain size[1], grain coordination[1], or grain boundary character[2]. However, many important processes, such as abnormal grain growth, initiation of stress-corrosion cracking, or fatigue, are often local phenomena and the full structure of individual grains and microstructural regions is important. Complete information about these phenomena may not be determined from two-dimensional (2-D) sections alone.

In recent years, 3-D reconstruction of serial sections has been used to determine grain shapes,[3-7] particle distributions,[3, 8-10] and the morphology of solidification structures.[3, 6] Serial sectioning combined with orientation imaging microscopy (OIM) obtained from electron backscatter diffraction (EBSD) data has been used to determine the grain boundary energy distribution in magnesia[11]. Recently, the dual-beam focused ion beam (FIB) scanning electron microscope (SEM) has been used to automate the collection of serial sections of OIM data[12-15]. This topic has recently been reviewed.[16] The 3-D FIB-OIM technique has mainly been employed to characterize metallic systems, and metallic systems with ceramic second-phases. Several studies have used the FIB to collect serial section images of ceramic materials[17-19], but the authors are unaware of any publications that have reported acquiring 3-D OIM data for a bulk ceramic with a FIB-SEM. In fact, it has not been entirely clear if this is practical or possible.

Ceramics offer some benefits as model materials for evaluating microstructural evolution. For example, grain boundary motion is typically driven only by capillarity, and it is often easy to produce fine-grained undeformed material directly from powder. Some examples of specific issues of interest in ceramic systems that need to be addressed in three dimensions include: the distribution, shapes, and connectivity of pores during the various stages of sintering, the shapes and aspect ratios of normal and abnormal grains, the grain boundary character and energy distributions of technologically important ceramics, and the effect of geometric factors on thermal stresses at interfaces.

Some of the problems associated with characterizing ceramics by 3-D FIB-OIM include: charging due to the low electrical conductivity of many ceramics, ion-induced beam damage that degrades EBSD image quality, preparation of the requisite sample geometry (needle, or pillar shape)[13, 20], and the low backscatter yield of some ceramics that have low average atomic weights (due to the large amount oxygen, nitrogen, carbon, etc. present). The most critical issue is charging, because distortion in the OIM data due to charging will make it impossible to align and register adjacent slices in the serial section, and may make the data unuseable. Materials with high bond strengths (such as many ceramics) can also take considerably longer to ion-mill than materials with much lower bond strengths, such as many metals. While many ceramics may be non-ideal candidates for 3-D OIM by FIB-SEM, the interest in characterizing them in this manner is considerable.

The current work evaluates the possibility of acquiring 3-D OIM data from the automated FIB-SEM technique. It describes a simple sample preparation procedure, acquisition parameters, and selected initial results that provide a basis for future work in this area.

EXPERIMENTAL PROCEDURE

Dense neodymia (Nd_2O_3) doped alumina samples were prepared as described elsewhere[21]. Samples of 8% yttria (Y_2O_3) stabilized Zirconia (ZrO_2) (YSZ), and magnesium aluminate spinel ($MgAl_2O_4$) were acquired from commercial sources. The grain size of the as-received spinel sample was sub-micron and the grains were coarsened at 1400^{o}C for 2 hours in order to facilitate collection of OIM data. Strontium titanate ($SrTiO_3$) (STO) was vacuum hot-pressed at 1200^{o}C for 2 hours and then annealed in air at 1200^{o}C for 2 hours.

Approximately needle shaped samples were prepared for the automated serial sectioning in the FIB-SEM (Nova 600, FEI company, Hillsboro, Or). It is important that the sample be shaped such that when material is milled away there is not adjacent material that will cause ‘shadowing’ of backscatter electrons traveling toward the EBSD detector. This geometry also minimizes re-deposition of the milled material. A schematic showing the sample preparation procedure is shown in Fig. 1. Samples were cut to less than 1mm thickness using a diamond impregnated blade on a low-speed saw. Both sides of the cut sample were polished to a 1 micron finish using diamond lapping films on a glass plate. Polishing was performed carefully such that a final thickness was in the range of ~20-60 μm. The samples were scored with a diamond tipped pen and snapped into triangular pieces. Both sides of the triangles were sputter-coated with ~2 nm of platinum. Having a needle geometry with both sides of the sample coated helps maximize the specific surface area of conducting surfaces. These pieces were 'glued' onto 45^{o} SEM pre-tilt stubs using conductive carbon paint (SPI, West Chester, Pa). On 45^{o} stubs, the samples can be tilted 7^{o} to 52^{o} towards the ion-column for ion-milling, or tilted 25^{o} to 70^{o} towards the EBSD detector (TexSEM, EDAX, Mahwah, NJ). The tips of the samples were ion milled in order to create a large flat area to scan for EBSD. Finally, circular feducial marks were milled into the samples. An example of a prepared needle of spinel is shown in Fig 2.

The serial section procedure requires that the sample be aligned accurately so that an equivalent amount of material is removed during each subsequent milling step. This is important to ensure that the spacing between each slice is accurate for reconstructing the data in 3-D. Automation was performed using a variant of the microscope control scripts originally developed by Uchic et al.[13] in the FEI runscript language. The samples were aligned using the circular fiducial markers along with pattern recognition software built into the FEI Nova system.

All samples were ion milled at 30 kV and 3 nA using a Ga^{+} ion beam. Electron backscattered diffraction data was acquired at 30 kV and 9.5 nA. It was found that the pattern quality increased with the electron beam accelerating voltage. At higher accelerating voltages backscattered electrons may originate from deeper within the sample, and increasing the voltage may help minimize the noise from surface damage induced by the ion-beam. Serial sections were reconstructed using the commercially available 3-D OIM visualization software (EDAX, Mahwah, NJ)

RESULTS AND DISCUSSION

Thirty consecutive layers of data were obtained for neodymia-doped alumina at a spacing of 150nm. Four slices of the data are shown in figure 3. The data was collected at a relatively low resolution due to the long collection times required (~5 points per second). Long exposure times were required for the collection of EBSD patterns both because alumina has a low average atomic weight, and the ion-beam induces damage in the surface which makes the patterns noisier than conventionally prepared samples. However, there is reasonable agreement between adjacent layers indicating that this system has the potential to be more thoroughly characterized using this 3-D FIB-OIM technique. Alumina may be considered a 'worst case scenario' for 3D FIB-OIM because of its low conductivity which makes it prone to charging under an electron beam, its high bond-strength, which makes it difficult to ion-mill, and its low average atomic weight, which produces a weak backscattered electron signal. The high tilt angles improve the yield of backscattered electrons, which helps reduce charging. It is also expected that the gallium contamination from the ion beam left on the scanned surface may contribute to electrical conductivity. Finally, the geometry of the sample, a needle with high specific surface area that is platinum coated, may help reduce charging due to the short distance (~20 µm) between any point and a conducting platinum surface. The issues of a slow ion-milling rate and low intensity of backscattered diffraction patterns associated with alumina simply result in longer acquisition times.

Reconstructed data for 10 planar sections of the spinel sample are shown in Figs. 4a-b. The electron backscatter diffraction patterns from the spinel sample were difficult to index due to a pseudosymmetry effect [22]. Relative to a traditionally prepared sample, the EBSD pattern quality is slightly diminished due to ion-beam induced damage, which makes this pseudosymmetry more difficult to detect. However, a single grain is selected and shown in Fig. 4b, and it appears to be a reasonably equiaxed grain. It should be noted that because the grains are made of cube-shaped voxels, the grain boundary planes are rough on the scale of the section depth and orientation resolution. To accurately determine the orientations of the grain boundary planes, it will be necessary to refine the alignment procedure (for example, see reference 16) and smooth the interface planes.

Reconstructed data for 21 planar sections of YSZ are shown in Figs. 5a-c. It may be seen from Fig. 4 that the registry between adjacent layers is good. This may also be seen in a cross-section shown in Fig. 5b. Individual grains are selected and shown in Fig. 5c, and it may be seen that these grains are relatively equiaxed. Reconstructed data for STO is shown in figure 6. This data is also well aligned and the grains appear to be equiaxed. These encouraging results indicate that it is possible to collect 3-D OIM data in the FIB-SEM for a variety of ceramic materials. This provides many new opportunities for characterizing and analyzing ceramic microstructures.

CONCLUSIONS

The results indicate that it is possible to acquire 3-D OIM data of ceramics using automation in the FIB-SEM. Encouraging results were obtained for alumina, magnesium aluminate spinel, and yttria-stabilized zirconia. Reliable 3-D reconstruction of the planar sections is possible in these materials, which presents new possibilities for characterizing ceramic microstructures.

ACKNOWLEDGEMENT

This work was supported the Pennsylvania DCED and by the MRSEC program of the National Science Foundation under Award Number DMR-0520425.

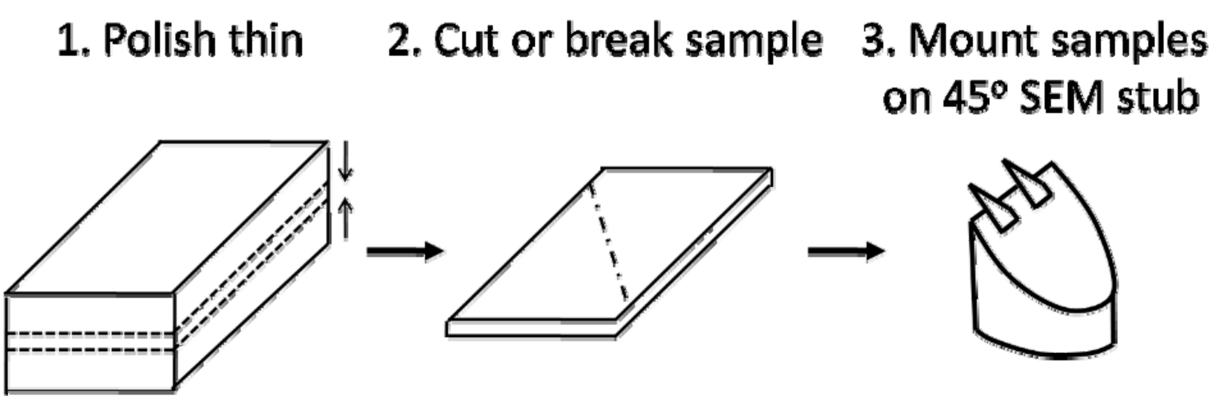

Figure 1: schematic of the sample preparation procedure

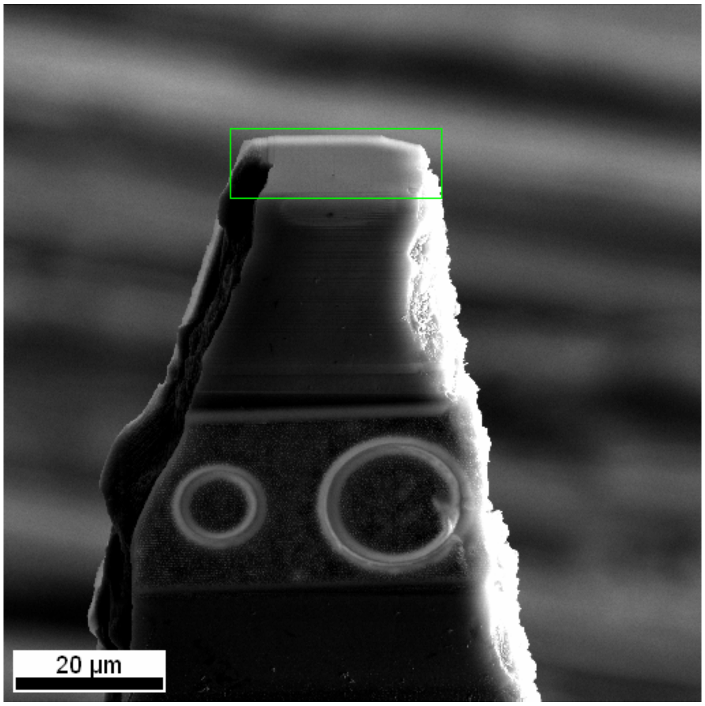

Figure 2: Image of a spinel sample with the EBSD scan area outlined (rectangular box), and circular fiducial markers.

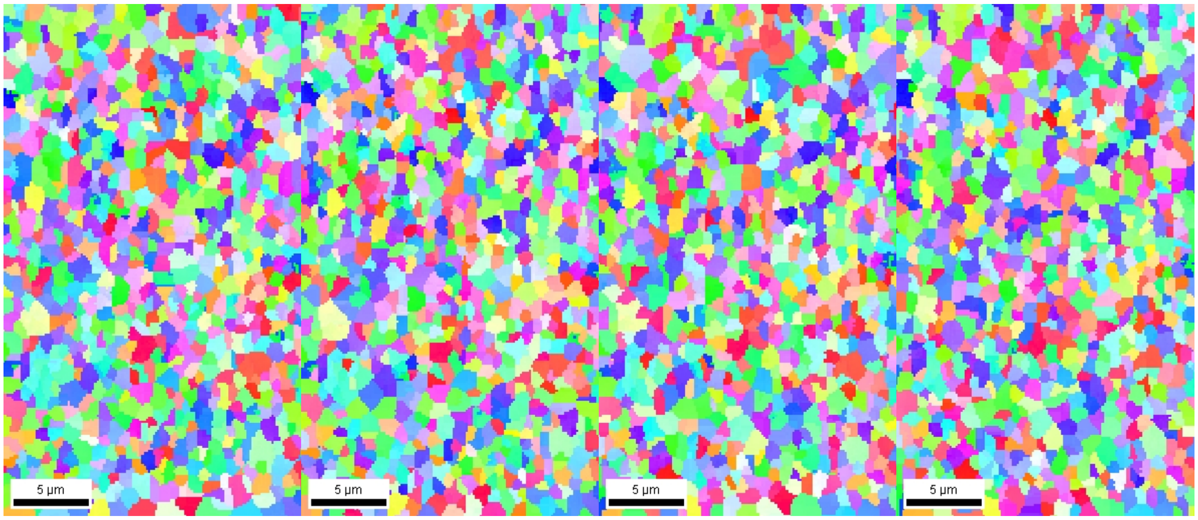

Figure 3: Orientation image maps of 4 consecutive serial sections of submicron alumina. The thickness between slices is 150nm.

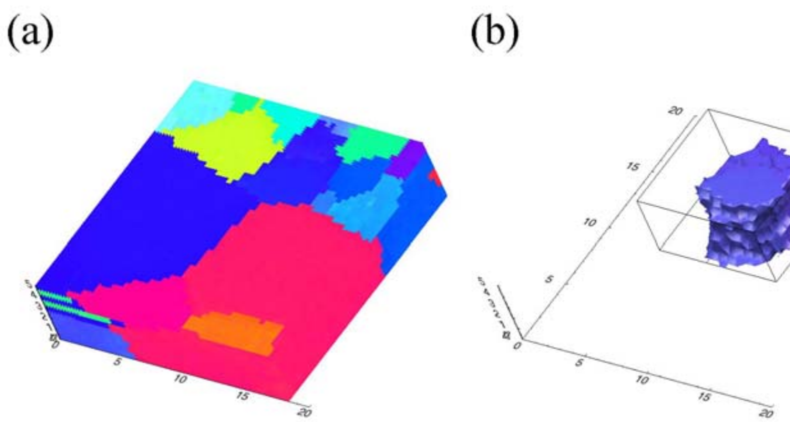

Figure 4: Reconstructed inverse pole figure data for spinel showing (a) several grains and (b) an individual selected grain.

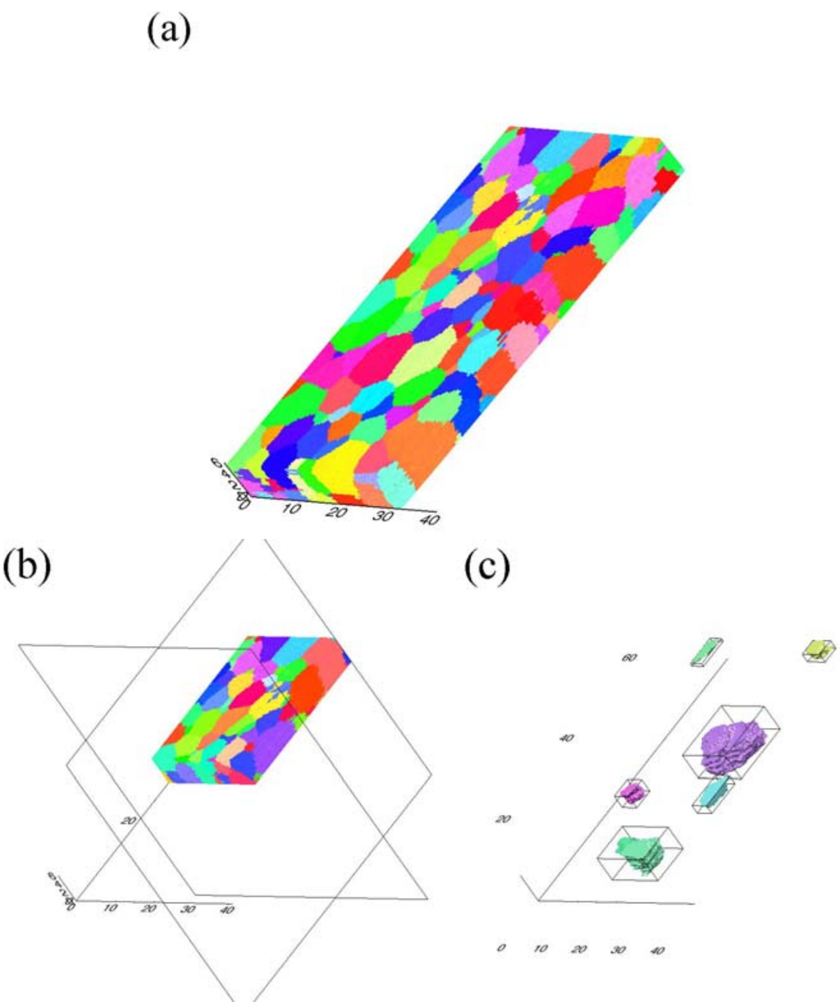

Figure 5: Reconstructed inverse pole figure data for YSZ showing (a) several planar sections reconstructed, (b) the same data cross-sectioned, and (b)several individual selected grains.

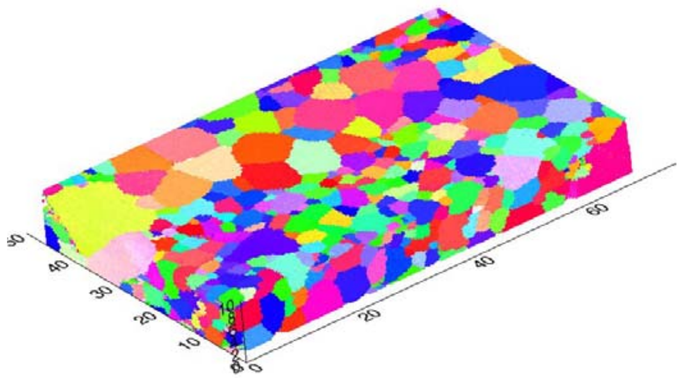

Figure 6: Reconstructed inverse pole figure data from 26 slices of a STO sample.

REFERENCES

1. R. T. Dehoff and J. Russ, *Practical Stereology,* 2 ed. (Springer, 2001).
2. D. Saylor, B. El-Dasher, B. Adams, and G. Rohrer, "Measuring the five-parameter grain-boundary distribution from observations of planar sections," Metallurgical and Materials Transactions A **35**(7), 1981-1989 (2004).
3. M. A. Dudek and N. Chawla, "Three-dimensional (3D) microstructure visualization of LaSn3 intermetallics in a novel Sn-rich rare-earth-containing solder," Materials Characterization **In Press, Corrected Proof**.
4. M. Frary, "Determination of three-dimensional grain boundary connectivity from two-dimensional microstructures," Scripta Materialia **57**(3), 205-208 (2007).
5. D. J. Rowenhorst, A. Gupta, C. R. Feng, and G. Spanos, "3D Crystallographic and morphological analysis of coarse martensite: Combining EBSD and serial sectioning," Scripta Materialia **55**(1), 11-16 (2006).
6. R. S. Sidhu and N. Chawla, "Three-dimensional microstructure characterization of Ag3Sn intermetallics in Sn-rich solder by serial sectioning," Materials Characterization **52**(3), 225-230 (2004).
7. B. J. Inkson, M. Mulvihill, and G. Mobus, "3D determination of grain shape in a FeAl-based nanocomposite by 3D FIB tomography," Scripta Materialia **45**(7), 753-758 (2001).
8. C. M. Dinnis, J. A. Taylor, and A. K. Dahle, "As-cast morphology of iron-intermetallics in Al-Si foundry alloys," Scripta Materialia **53**(8), 955-958 (2005).

9. M. Li, S. Ghosh, T. N. Rouns, H. Weiland, O. Richmond, and W. Hunt, "Serial Sectioning Method in the Construction of 3-D Microstructures for Particle-Reinforced MMCs," Materials Characterization **41**(2-3), 81-95 (1998).
10. S. I. Lieberman, A. M. Gokhale, and S. Tamirisakandala, "Reconstruction of three-dimensional microstructures of TiB phase in a powder metallurgy titanium alloy using montage serial sectioning," Scripta Materialia **55**(1), 63-68 (2006).
11. D. M. Saylor, A. Morawiec, and G. S. Rohrer, "Distribution and Energies of Grain Boundaries in Magnesia as a Function of Five Degrees of Freedom," Journal of the American Ceramic Society **85**(12), 3081-3083 (2002).
12. J. Konrad, S. Zaefferer, and D. Raabe, "Investigation of orientation gradients around a hard Laves particle in a warm-rolled Fe3Al-based alloy using a 3D EBSD-FIB technique," Acta Materialia **54**(5), 1369-1380 (2006).
13. M. D. Uchic, M. A. Groeber, D. M. Dimiduk, and J. P. Simmons, "3D microstructural characterization of nickel superalloys via serial-sectioning using a dual beam FIB-SEM," Scripta Materialia **55**(1), 23-28 (2006).
14. W. Xu, M. Ferry, N. Mateescu, J. M. Cairney, and F. J. Humphreys, "Techniques for generating 3-D EBSD microstructures by FIB tomography," Materials Characterization **58**(10), 961-967 (2007).
15. N. Zaafarani, D. Raabe, R. N. Singh, F. Roters, and S. Zaefferer, "Three-dimensional investigation of the texture and microstructure below a nanoindent in a Cu single crystal using 3D EBSD and crystal plasticity finite element simulations," Acta Materialia **54**(7), 1863-1876 (2006).
16. A. D. Rollett, S.-B. Lee, R. Campman, and G. S. Rohrer, "Three-Dimensional Characterization of Microstructure by Electron Back-Scatter Diffraction," Annual Review of Materials Research **37**, 627-658 (2007).
17. L. Holzer, B. Muench, M. Wegmann, P. Gasser, and R. J. Flatt, "FIB-nanotomography of particulate systems-part I: particle shape and topology of interfaces," Journal of the American Ceramic Society **89**(8), 2577-2585 (2006).
18. J. R. Wilson, W. Kobsiriphat, R. Mendoza, H.-Y. Chen, J. M. Hiller, D. J. Miller, K. Thornton, P. W. Voorhees, S. B. Adler, and S. A. Barnett, "Three-dimensional reconstruction of a solid oxide fuel cell anode," Nature Materials **5**(7), 541-544 (2006).
19. H. Z. Wu, S. G. Roberts, G. Mobus, and B. J. Inkson, "Subsurface damage analysis by TEM and 3D FIB crack mapping in alumina and alumina/5 vol.% SiC nanocomposite," Acta Materialia **51**(1), 149-163 (2003).
20. M. Schaffer and J. Wagner, "Block lift-out sample preparation for 3D experiments in a dual beam focused ion beam microscope," Microchimica Acta.
21. S. J. Dillon, M. Tang, W. C. Carter, and M. P. Harmer, "Complexion: A New Concept for Kinetic Engineering in Materials Science," Acta Materialia **55**(18), 6208-6218 (2007).
22. E. Chuprunov, "Fedorov pseudosymmetry of crystals: Review," Crystallography Reports **52**(1), 1-11 (2007).